Journal of Alloys and Compounds 522 (2012) 101–105

Contents lists available at SciVerse ScienceDirect

Journal of Alloys and Compounds

journal homepage: www.elsevier.com/locate/jallcom

High-pressure synthesis of $Na_{1-x}Li_xMgH_3$ perovskite hydrides

R. Martínez-Coronado [a,*], J. Sánchez-Benítez [a,b], M. Retuerto [c], M.T. Fernández-Díaz [d], J.A. Alonso [a]

[a] Instituto de Ciencia de Materiales de Madrid, C.S.I.C., Cantoblanco, E-28049 Madrid, Spain
[b] Dpto. Química Física I, Facultad de Ciencias Químicas, Universidad Complutense de Madrid, 28040 Madrid, Spain
[c] Department of Chemistry and Chemical Biology, Rutgers, The State University of New Jersey, 610 Taylor Road, Piscataway, NJ 08854-808, USA
[d] Institut Laue Langevin, BP 156X, Grenoble F-38042, France

ARTICLE INFO

Article history:
Received 19 October 2011
Received in revised form 10 January 2012
Accepted 16 January 2012
Available online 28 January 2012

Keywords:
Metal hydrides
$NaMgH_3$
Neutron powder diffraction
High-pressure synthesis

ABSTRACT

Magnesium base alloys are very attractive for hydrogen storage due to their large hydrogen capacity, small weight and low-cost. We have designed a new synthesis method for the ternary metal hydride perovskite system $Na_{1-x}Li_xMgH_3$, based on the direct reaction of simple hydrides under high-pressure and moderate-temperature conditions. Well-crystallized samples were obtained in a piston-cylinder hydrostatic press at moderate pressures of 2 GPa and temperatures around 750 °C from mixtures of MgH_2, NaH and LiH enclosed in gold capsules. X-ray and neutron powder diffraction analysis were used to identify the purity of the samples and provide an accurate description of the crystal structure features ($GdFeO_3$ type). $Na_{1-x}Li_xMgH_3$ hydrides series ($0 \leq x \leq 0.18$) show an orthorhombic symmetry with space group P*nma* (No. 62). Thermogravimetric analysis (TGA) and differential scanning calorimetry (DSC) have been carried out to determine the hydrogen desorption temperatures.

1. Introduction

Ternary compounds with perovskite structure ABX_3 have been exhaustively investigated over the last fifty years, due to their astonishingly varied panoply of properties, including dielectric, electronic, magnetic and optical phenomena. Most of the better known materials are oxides (X = O), for which the crystal chemistry has been deeply studied in connection with the properties of interest. Much less scarce are the perovskites containing hydrogen ions at the X sublattice. Some of them have been recently described, and immediately attracted the attention of the sustainable technologies community [1], since they can be used as hydrogen storage materials. In particular, ternary hydrides between magnesium and alkali elements are particularly good candidates for advanced hydrogen storage systems, due to their light weight and low cost [2]. The perovskite-type hydrides composed of light elements are expected to present as much as twice energy density as the conventional ones, based upon $LaNi_5$ alloys. The perovskite hydrides are formulated as ABH_3, where A and B are monovalent and divalent cations, respectively [3–5]. Thus, most of the perovskite-type hydrides are mainly composed by 1A group elements and 2A group elements of the periodic table. In the Mg-based perovskite-type hydrides, $AMgH_3$ (A = Na, K, Rb), the main types of structural distortion described in perovskite-oxide have been identified [6]. For instance, $NaMgH_3$ [7] has an orthorhombic perovskite structure analogous to the $GdFeO_3$ type (space group P*nma*) which is common in low tolerance factor oxide perovskites, where the singly charged Na cation occupies eight-fold coordinated voids. Along the series of hydrides $NaMgH_3$, $KMgH_3$, and $RbMgH_3$ [8–10] a progressive structural distortion is observed; $NaMgH_3$ is orthorhombic as mentioned, $KMgH_3$ is reported to occur in the ideal cubic perovskite structure, while $RbMgH_3$ has a non-ferroelectric hexagonal $P6_3/mmc$ structure, of the type seen in some high tolerance factor oxides and fluorides [11].

The usual procedure to prepare metal hydrides is by hydrogenation of metal alloys, for instance, $TiFe_{1-x}M_x$ (M = Co, Ni, or Al, $x \leq 0.5$) intermetallic samples were prepared in an arc furnace under an argon atmosphere and then hydrogenated by exposing them to 5.0 MPa H_2 at room temperature for several cycles [12]. An alternative, traditional method is the mechanochemical synthesis, by high-energy ball-milling under H_2, which presents several disadvantages since (i) the sample can be easily polluted by the steel balls, (ii) the sample can be easily oxidized in air, (iii) the reaction times are, in general, very long and (iv) the obtained samples exhibit a poor crystallization, which make them not suitable for a complete structural characterization. Concerning $NaMgH_3$ and related hydrides, they have been synthesized by heating mixtures composed of NaH and Mg (or MgH_2) in a molar ratio Na:Mg = 1:1 [1,7,13]. Ternary hydrides were obtained by sintering or melting methods at temperatures lower than 500 °C and under a hydrogen pressure between 10 and 200 bar, at temperatures spanning from 400 °C to 480 °C [4,7,14,15].

* Corresponding author. Tel.: +34 91 334 9000; fax: +34 91 372 0623.
E-mail address: rmartinez@icmm.csic.es (R. Martínez-Coronado).

0925-8388/$ – see front matter © 2012 Elsevier B.V. All rights reserved.
doi:10.1016/j.jallcom.2012.01.097

Solid-state high-pressure synthesis is a powerful and effective technique to explore new compounds in a variety of research areas. In the field of the hydrogen storage materials, this method is being used recently to obtain new hydrides as a different approach from traditional methods [16]. The aim of the present study was to investigate the formation of $NaMgH_3$ under hydrostatic pressure conditions at moderate temperatures, as well as the formation of new Li-substituted derivatives with nominal composition $Na_{1-x}Li_xMgH_3$ ($x = 0$, 0.25 and 0.5). The replacement of Na by Li would be advantageous for the hydrogen storage ability of the parent material [17,18] since (i) Li is lighter than Na, so the amount of hydrogen per hydride mass should be improved and (ii) the stability of the Li perovskite is found to be lower, therefore the hydrogen desorption proceeds at lower temperatures. In this work we describe a comprehensive study of the crystal structure and thermal analysis of the $Na_{1-x}Li_xMgH_3$ series, prepared by the mentioned high-pressure method.

2. Experimental procedure

Pollycrystalline samples of nominal composition $Na_{1-x}Li_xMgH_3$, $x = 0$, 0.25 and 0.5 were prepared from stoichiometric mixtures of MgH_2, NaH and LiH. The reactants were intimately mixed and ground in a glove box under N_2 atmosphere. This mixture was placed into a gold capsule (8 mm diameter, 10 mm length), sealed inside the glove box and then set into a cylindrical graphite heater (10 mm internal diameter). The reaction took place in a piston-cylinder press (Rockland Research Co.), at a moderate reaction pressure (2 GPa) and temperature (750 °C), for short reactions times of less than 1 h. Then, the products were quenched under pressure. The ramp-up for the material synthesis is rather fast, near 150 °C min^{-1}; we reach 750 °C in approximately 5 min. The ramp-down is a quenching process; in a matter of seconds the sample is quenched from 750 °C down to RT. We found these optimal synthesis conditions after performing several experiments upon different conditions (temperature, starting materials, synthesis time, etc.).

The initial characterization was carried out by X-ray diffraction (XRD) with a Bruker-axs D8 Advanced diffractometer (40 kV, 30 mA), controlled by a DIFFRACT^{PLUS} software, in Bragg–Brentano reflection geometry with Cu K_α radiation ($\lambda = 1.5418$ Å) and a PSD (Position Sensitive Detector). A filter of nickel allows the complete removal of Cu K_β radiation. For the study of the crystal structure, neutron powder diffraction (NPD) experiments were carried out in the high-resolution powder diffractometer D2B at the Institut Laue-Langevin at Grenoble, with a wavelength of 1.594 Å. The patterns were collected at room temperature. About 0.8 g of sample was contained in a vanadium can, and a time of 3 h was required to collect a full diffraction pattern. The NPD data were analyzed by the Rietveld method [19] with the FULLPROF program [20]. A pseudo-Voigt function was chosen to generate the line shape of the diffraction peaks. The following parameters were refined in the final run: scale factor, background coefficients, zero-point error, pseudo-Voigt corrected for asymmetry parameters, positional coordinates and isotropic thermal factors for all the atoms. The coherent scattering lengths for Na, Li, Mg and H were 3.63, −1.90, 5.375 and −3.739 fm, respectively.

Thermal analysis was carried out in a Mettler TA3000 system equipped with a TC10 processor unit. Thermogravimetric (TGA) curves were obtained in a TG50 unit, working at a heating rate of 10 °C min^{-1}, in a reducing $H_2(5\%)/N_2(95\%)$ flow of 0.3 L min^{-1}. About 50 mg of sample were used for each experiment. Differential Scanning Calorimetry (DSC) experiments were performed in a DSC30 unit, in the temperature range of 35–500 °C. The heating rate was 10 °C min^{-1}, using about 70 mg of sample in each run.

3. Results and discussion

3.1. Crystal structure

The samples were prepared under an external hydrostatic pressure of 2 GPa. The x-ray diffraction patterns of the $Na_{1-x}Li_xMgH_3$ hydrides show sharp and well-defined reflections, as shown in Fig. 1. The samples present a high crystallinity, in contrast with the compounds obtained by the traditional ball-milling method. This feature is important in order to determine the nature and proportion of the different phases present in the patterns, refined by the Rietveld method, and to define some structural peculiarities. The diffraction peaks of unreacted MgH_2 and MgO were detected in the samples with nominal compositions $x = 0.25$ and 0.5 (♦ and ○ symbols in Fig. 1, respectively). Excess Li is not observed by XRD, probably because it is eventually present as an amorphous phase.

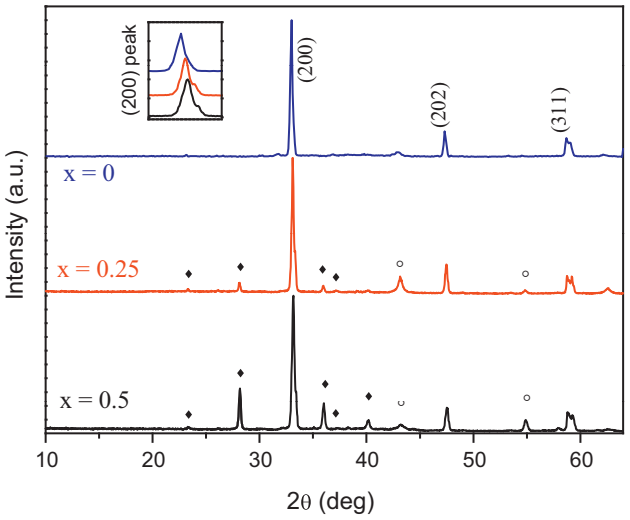

Fig. 1. XRD patterns of $Na_{1-x}Li_xMgH_3$ hydrides prepared by high-pressure techniques. The indexed peaks correspond to ♦ MgH_2 and ○ MgO.

In the $NaMgH_3$ pattern, the Bragg reflections were identified to be those belonging to a distorted perovskite structure. These peaks, corresponding to the main phase structure, shift to higher diffraction angles as Na atoms are replaced by Li (inset of Fig. 1). This is due to the smaller size of the Li cations, which initially confirmed that Li ions are incorporated into the perovskite crystal structure.

In order to carry out a more accurate structural study and also to identify, locate and quantify light atoms as H and Li, we performed a neutron powder diffraction investigation at room temperature for all the samples. NPD on hydrides (instead of deuterides) is possible nowadays owing to the availability of better neutron diffraction facilities. Henry and Weller have demonstrated the possibilities and limits of NPD on ^1H (protium) in much detail [21–23]. Despite the incoherent scattering of H, good NPD patterns were collected in the present case, showing an excellent crystallinity for the samples. The analysis of the obtained data confirms the perovskite structure for the $Na_{1-x}Li_xMgH_3$ hydrides with *Pnma* space group (No. 62), corresponding to the orthorhombically distorted $GdFeO_3$ type. In this setting, the Na/Li cations are placed at 4*c* (x, 1/4, z) sites, the Mg cations at 4*b* (0, 0, 1/2) sites, and the two kinds of nonequivalent hydrogen atoms (H1 and H2) at 4*c* (x, 1/4, z) and at 8*d* (x, y, z) sites, respectively.

Fig. 2 illustrates the good agreement between the observed and calculated NPD patterns at room temperature for $Na_{1-x}Li_xMgH_3$ hydrides and Table 1 summarizes the unit-cell, atomic, thermal parameters and discrepancy factors after the Rietveld refinements of the crystal structures. The lattice parameters of the $Na_{1-x}Li_xMgH_3$ hydrides decrease as the amount of Li increases, as shown in Fig. 3a, being the shrinkage more pronounced along the *c* axis. It is due to the smaller ionic size of Li^+ respect to the replaced Na^+ ions. This effect can clearly be seen in the reduction of the unit-cell volume along the series (Fig. 3b). The occupancy factors for Na/Li as well as for H atoms were refined in order to obtain the stoichiometric formula for each compound; the results are included in Table 1. After the final refinement, the crystallographic formulae for the three ternary hydrides are $NaMgH_{3.0}$, $Na_{0.95}Li_{0.05}MgH_{2.73}$ and $Na_{0.82}Li_{0.18}MgH_{2.58}$. The hydrogen deficiency found in the Li-containing samples can be due to H desorption from the sample after their synthesis. The maximum Li content in the samples was 0.18 (for nominal $x = 0.5$), indicating the difficulty of Li atoms to be introduced in this system.

Table 2 contains the main interatomic distances and angles. The MgH_6 octahedra maintain a nearly ideal configuration with

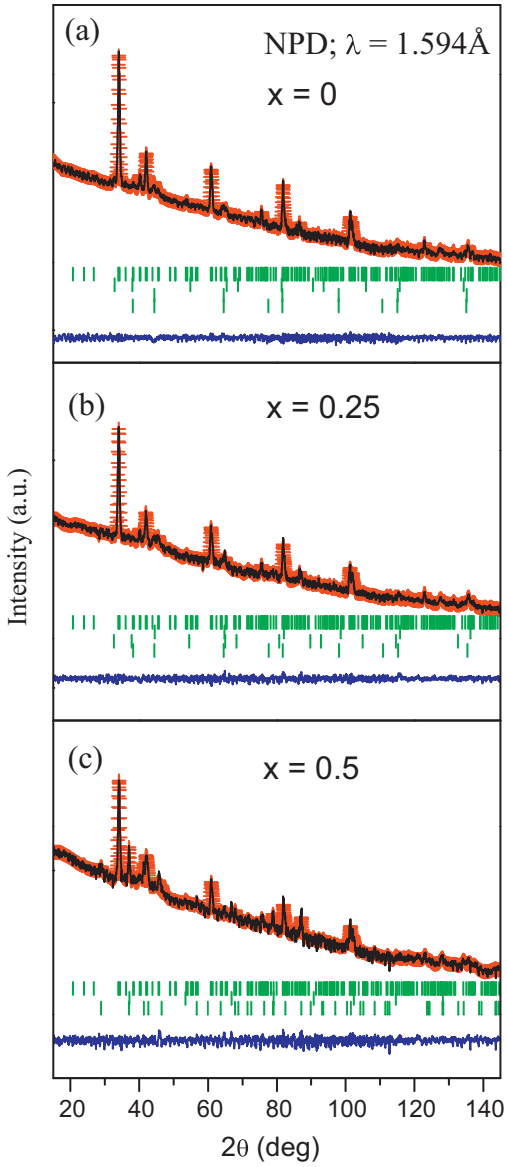

Fig. 2. Comparison of the observed (crosses), calculated (solid line), and difference (at the bottom) NPD patterns for (a) $x = 0$, (b) $x = 0.25$, and (c) $x = 0.5$ (nominal compositions) at $T = 295$ K. The three series of tick marks correspond to the positions of the allowed Bragg reflections for the main phase, MgH_2 and MgO.

similar Mg—H bond length, and the tilting of the MgH_6 units leads to a distorted cuboctahedral environment for the Na^+/Li^+ cations. The distortion mechanism is a tilting of essentially rigid MgH_6 octahedra. It occurs when the A-site cation is too small for its 12-coordinated cavity in the cubic perovskite structure. The tilting angle (⟨Mg—H—Mg⟩) decreases as x increases, as shown in Fig. 3c, from 155.12° for $NaMgH_3$ to 153.64° for $Na_{0.82}Li_{0.18}MgH_{2.58}$, indicating that the structure is more distorted as Li is introduced at A positions.It is interesting to compare the present description of the crystal structure of $NaMgH_3$ with precedent determinations. Bouamrane et al. [7] described very distorted MgH_6 octahedra, with individual distances Mg—H2 of 2.237 Å and 1.7521 Å; our data (Table 2) show much more regular octahedra with Mg—H2 distances of 1.958(1) Å and 1.971(1) Å. Along the $Na_{1-x}Li_xMgH_3$ series we observe a progressive distortion of the MgH_6 octahedron, to reach Mg—H2 bond-lengths of 2.001(1) Å and 1.937(2) Å for $x = 0.18$, as a consequence of the structural distortion induced by Li as it is incorporated into the crystal structure. Ikeda et al. [24]

Table 1
Unit-cell and thermal parameters for $Na_{1-x}Li_xMgH_3$ in orthorhombic *Pnma* (No. 62) space group, from NPD at 295 K. (Na, Li) are placed at 4*c* (x, 1/4, z), (Mg) at 4*b* (0, 0, 1/2), H1 at 4*c* (x, 1/4, z) and H2 at 8*d* (x, y, z) positions.

Nominal composition	$x = 0$	$x = 0.25$	$x = 0.5$
a (Å)	5.4651(6)	5.4656(5)	5.460(1)
b (Å)	7.7026(9)	7.7024(8)	7.698(2)
c (Å)	5.4135(6)	5.4065(6)	5.399(1)
V (Å^3)	227.88(4)	227.61(4)	226.96(9)
Na/Li 4*c* (x, 1/4, z)			
x	0.0154(4)	0.0169(5)	0.0121(1)
z	−0.0084(5)	0.0000(6)	−0.003(1)
B_{iso}	2.31(2)	2.53(4)	1.01(6)
Na/Li f_{occ}	1.0	0.962(1)/0.038(1)	0.824(1)/0.176(1)
Mg 4*b* (0, 0, 1/2)			
B_{iso}	0.843(8)	0.43(1)	1.43(3)
f_{occ}	1.0	1.0	1.0
H1 4*c* (x, 1/4, z)			
x	0.4677(4)	0.4808(6)	0.499(1)
z	0.0808(3)	0.0845(4)	0.0878(5)
B_{iso}	2.56(3)	2.18(6)	-0.11(7)
f_{occ}	1.0	0.708(2)	0.568(2)
H2 8*d* (x, y, z)			
x	0.2858(2)	0.2912(2)	0.3014(4)
y	0.0367(1)	0.0367(1)	0.0311(3)
z	0.7119(2)	0.7136(2)	0.7061(4)
B_{iso}	2.34(2)	1.77(2)	3.24(5)
f_{occ}	1.0	1.0	1.0
Reliability factors			
χ^2	2.65	2.20	3.03
R_p (%)	1.33	1.19	1.35
R_{wp} (%)	1.76	1.54	1.80
R_{exp} (%)	1.10	1.06	1.04
R_I (%)	8.62	8.61	11.3

described extremely high displacement factors for hydrogen atoms of 5.0 Å^2 (unrefined); our present NPD data allowed us to refine these parameters, obtaining reasonable values between 2 and 3 Å^2 (see Table 1). As observed before [7,24], the Mg displacement factors take moderate values around 0.8 Å^2.

In ABH_3 hydride perovskites, the tolerance factor has been used to predict their structural types assuming a constant size of H^- ions, i.e. 1.3 Å or 1.4 Å [4,7]. Although this assumption is generally valid for oxides, it is problematic for hydrides. In contrast to O^{2-} or halide anions, which usually assume nearly constant radii, hydrides show a diffuse and non-spherical character of the electron distribution around H. In the $AAeH_3$ (Ae = alkali-earth ion) perovskite hydrides, the H^- anion radius (coordination number = 6) can be derived from the M—H bond either in B-site octahedra or A-site cuboctahedra [25], but there is no constant size relationship for the different

Table 2
Selected atomic distances (Å) and angles (deg) for $Na_{1-x}Li_xMgH_3$ at 295 K.

Nominal composition	$x = 0$	$x = 0.25$	$x = 0.5$
Distances (Å)			
(Na/Li)—H1	2.519(3)	2.576(5)	2.703(6)
—H1	2.329(3)	2.255(4)	2.244(6)
(Na/Li)—H2 (x2)	2.679(2)	2.710(3)	2.791(5)
—H2 (x2)	2.342(2)	2.357(2)	2.316(4)
—H2 (x2)	2.735(2)	2.704(3)	2.645(4)
⟨Na/Li—H⟩	2.545	2.547	2.556
Mg—H1 (x2)	1.9826(5)	1.9820(6)	1.9823(8)
Mg—H2 (x2)	1.958(1)	1.987(1)	2.001(1)
—H2 (x2)	1.971(1)	1.944(1)	1.937(2)
⟨Mg—H⟩	1.971	1.971	1.973
Angles (°)			
Mg—H1—Mg	152.43(3)	152.61(3)	152.29(6)
Mg—H2—Mg (x2)	156.44(4)	155.85(5)	154.31(10)
⟨Mg—H—Mg⟩	155.12	154.77	153.64

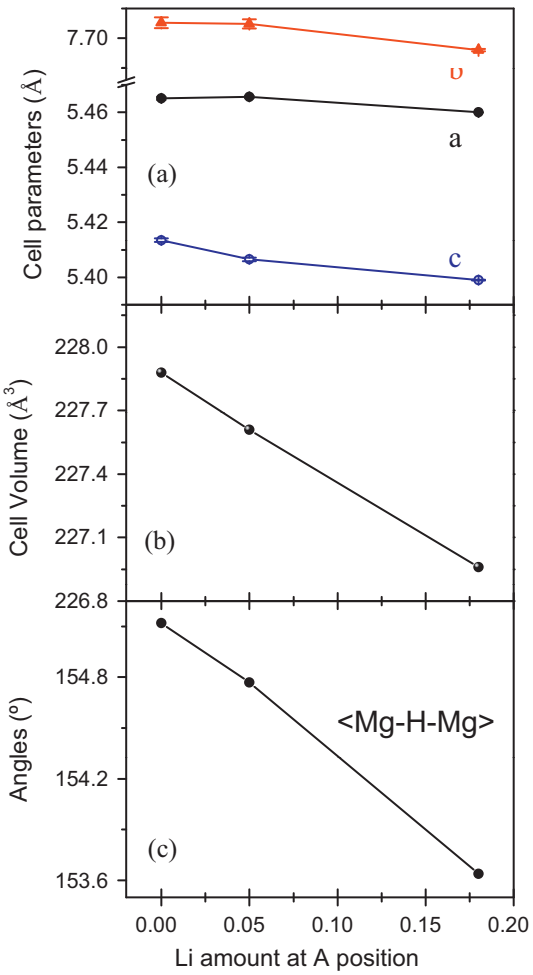

Fig. 3. Variation of (a) the unit-cell parameter, (b) cell volume, and (c) ⟨Mg—H—Mg⟩ tilting angle for $Na_{1-x}Li_xMgH_3$ as a function of the actual amount of Li at the A position of the perovskite.

cation species. For instance, from the ⟨Mg—H⟩ distance observed for $NaMgH_3$, of 1.971 Å, we obtain a size for H^- of 1.25 Å (assuming $r(^{VI}Mg^{2+}) = 0.72$ Å [26]). However, from the average ⟨Na—H⟩ distances of 2.545 Å we obtain a size for H^- of 1.37 Å (assuming $r(^{VIII}Na^+) = 1.18$ Å [26]). The large H^- anion size derived from Na—H bond can presumably be explained by the polyhedral tilting.

On the other hand, as the tolerance factor (t) is a geometrical parameter based on rigid spheres of constant radius, in the case of hydrides the polarization of H^- and the covalence of the M—H bond should also be considered. Using a constant H^- radius of 1.3 Å, we determined that the tolerance factor for $NaMgH_3$ is $t = 0.87$. As we replace Na by Li, the tolerance factor decreases. When the covalence effect on shortening of the Li—H bond length is considered, the tolerance factor will be even smaller, reducing the stability for a perovskite. Indeed no perovskite structure was found in the Li–Mg–H system ($t = 0.77$), and we found a maximum Li incorporation level of $x = 0.18$. In fact, the crystal structure of the hypothetical $LiMgH_3$ hydride has been predicted from ab-initio calculations [27], and the most stable arrangement has been found to be the trigonal $LiTaO_3$-type (R3c space group) structure, which contains highly distorted octahedra.

3.2. Thermal analysis (TGA and DSC)

The thermal stability was studied by recording the TGA curves, in order to determine the hydrogen contents and the desorption temperatures. The measurements were performed in a H_2/N_2 (5%/95%) flow. The quantity of desorbed hydrogen is always calculated from the weight loss between the weight sample at room temperature and the weight sample at the minimum of the peak, corresponding to the highest rate of weight loss. Fig. 4a shows the normalized TGA curves for all the samples prepared. It is possible to determine an approximate value of the hydrogen desorption temperature using the first derivative of the curves. Table 3 shows the desorption temperatures obtained from these curves for the studied samples, in the temperature range between 413 and 435 °C. It is important to highlight that the desorption temperature decreases along the series as Li ions are introduced in the compounds, which is certainly related with the lower stability of the hydrides as the tolerance factor of the perovskite structure diminishes when Li is incorporated at the A positions. In fact, a theoretical approach [8] finds out that Li substitution of Na in $NaMgH_3$ linearly reduces the dehydrogenation reaction enthalpy and may result in a favorable modification of the thermodynamics. The obtained calculation suggests that Li substitution in $NaMgH_3$ may result in a favorable modification for onboard hydrogen storage application, which is in the line of the present results.

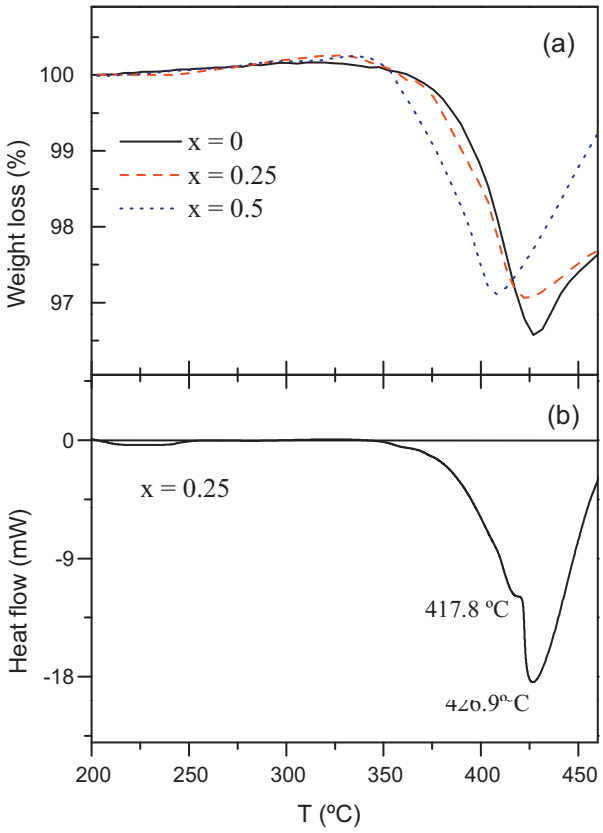

Fig. 4. (a) TGA and (b) DSC curves for $Na_{1-x}Li_xMgH_3$, obtained under a H_2/N_2 (5%/95%) flow.

Table 3 also shows the quantity of desorbed hydrogen that corresponds to the hydrogen capacity of each sample. The values of hydrogen loss are in between 1.39 and 1.76 H atom/formula compared to the ideal 3 H atoms/formula. This difference is attributed to the fact that the decomposition of the compounds into the

Table 3
Desorption temperatures and amount of desorbed hydrogen for $Na_{1-x}Li_xMgH_3$.

Nominal composition	$x = 0$	$x = 0.25$	$x = 0.5$
H loss (at./formula)	1.76	1.41	1.39
H (wt.%)	3.41	2.95	2.82
T desorp. (°C)	435	427	413

elemental Na, Li and Mg [23] is followed, almost in parallel, with the subsequent oxidation of these elements to the corresponding oxides, even in the presence of a reducing H_2/N_2 flow, since the TGA equipment is not perfectly sealed. The oxidation at elevated temperatures (above 400–425 °C) is clearly observed in the TGA curves as a continuous weight gain which is probably superimposed to the H release, masking the net value of the hydrogen capacity.

Differential scanning calorimetry (DSC) was also used to observe the phase transition connected to the thermal dehydrogenation of the samples. We used a H_2/N_2 (5%/95%) flow to avoid oxidation of the samples. As it is shown in Fig. 4b for nominal $x = 0.25$ perovskite, there is an endothermic peak associated with the desorption of H in the sample. The decomposition (desorption) temperature obtained by DSC is around 420 °C. It takes place in two steps (first step: $NaMgH_3 \rightarrow NaH + Mg + H_2$ and second step: $NaH + Mg + H_2 \rightarrow Na + Mg + 3/2H_2$), as it has been previously reported by Ikeda et al. [22]. The desorption temperatures observed in the TGA curves (Table 3) are in good agreement with the values found out from the DSC experiments.

4. Conclusions

We have prepared, by an original synthesis procedure, the ternary hydrides $Na_{1-x}Li_xMgH_3$ in one single step using a high-pressure technique in a very short reaction time and moderate temperatures. This high-pressure method produces well-crystallized samples in contrast with the compounds obtained by the traditional ball-milling technique. The direct structural characterization of the hydrides by NPD has been possible in spite of the H incoherent scattering. The crystal structure corresponds to an orthorhombic superstructure of perovskite, defined in the *Pnma* space group for all the compounds. As Li is introduced in the system, the unit-cell parameters decrease, the tilting angle increases and the MgH_6 octahedra become more distorted due to the smaller ionic size of Li^+ *vs* Na^+. The hydrogen desorption temperature determined from thermogravimetric and DSC analysis, in the 413–435 °C range, decreases as Li is introduced into the structure, due to the lower structural stability of the Li-containing perovskites.

Acknowledgements

We thank the financial support of the Spanish Ministry of Science and Innovation to the project MAT2010-16404 and of the Comunidad de Madrid to the project S2009PPQ-1551. We are grateful to the Institut Laue-Langevin (ILL) in Grenoble for making all facilities available.

References

[1] E. Rönnebro, D. Noréus, K. Kadir, A. Reiser, B. Bogdanovic, J. Alloys Compd. 299 (1–2) (2000) 101–106.
[2] H. Fujii, T. Ichikawa, Physica B 383 (2006) 45.
[3] A. Zaluska, L. Zaluski, J.O. Ström-Olsen, J. Alloys Compd. 307 (1–2) (2000) 157.
[4] F. Gingl, T. Vogt, E. Akiba, K. Yvon, J. Alloys Compd. 282 (1999) 125.
[5] B. Bertheville, T. Herrmannsdörfer, K. Yvon, J. Alloys Compd. 325 (2001) L13.
[6] K. Komiya, N. Morisaku, R. Rong, Y. Takahashi, Y. Shinzato, H. Yukawa, M. Morinaga, J. Alloys Compd. 453 (2008) 157–160.
[7] A. Bouamrane, J.P. Laval, J.P. Soulie, J.P. Bastide, Mater. Res. Bull. 35 (2000) 545.
[8] X.-B. Xiao, B.-Y. Tang, S.-Q. Liao, L.-M. Peng, W.-J. Ding, J. Alloys Compd. 474 (1–2) (2009) 522–526.
[9] S. Geller, J. Chem. Phys. 24 (1956) 1236.
[10] A.J. Maeland, W.D. Lahar, Z. Phys. Chem. 179 (1993) 181.
[11] M. Fornari, A. Subedi, D.J. Singh, Phys. Rev. B 76 (2007) 214118.
[12] S.-M. Lee, T.-P. Perng, J. Alloys Compd. 291 (1–2) (1999) 254–261.
[13] S. Ono, H. Hayakawa, D. Tsubone, J. Ceram. Soc. Jpn. 86 (1978) 388.
[14] H.H. Park, M. Pezat, B. Darriet, P. Hagenmuller, Rev. Chim. Miner. 24 (1987) 525.
[15] G. Renaudin, B. Bertheville, K. Yvon, J. Alloys Compd. 353 (2003) 175.
[16] M. Retuerto, J. Sanchez-Benitez, E. Rodriguez-Cañas, D. Serafini, J.A. Alonso, Int. J. Hydrogen Energy 35 (2010) 7835–7841.
[17] K. Ikeda, Y. Nakamori, S. Orimo, Acta Mater. 53 (2005) 3453–3457.
[18] K. Ikeda, Y. Kogure, Y. Nakamori, S. Orimo, Solid State Chem. 35 (2007) 329–337.
[19] H.M. Rietveld, J. Appl. Crystallogr. 2 (1969) 65–71.
[20] J. Rodríguez-Carvajal, Physica B 192 (1993) 55–69.
[21] M.T. Weller, P.F. Henry, V.P. Ting, C.C. Wilson, Chem. Commun. (Cambridge, U.K.) (2009) 2973–2989.
[22] P.F. Henry, M.T. Weller, C.C. Wilson, Chem. Commun. (Cambridge, U.K.) (2008) 1557–1559.
[23] V.P. Ting, P.F. Henry, H. Kohlmann, C.C. Wilson, M.T. Weller, Phys. Chem. Chem. Phys. 12 (2010) 2083–2088.
[24] K. Ikeda, S. Kato, Y. Shinzato, N. Okuda, Y. Nakamori, A. Kitano, H. Yukawa, M. Morinaga, S. Orimo, J. Alloys Compd. 446–447 (2007) 162–165.
[25] H. Wu, W. Zhou, T.J. Udovic, J.J. Rush, T. Yildirim, J. Phys. Chem. C 113 (2009) 15091–15098.
[26] R.D. Shanon, Acta Crystallogr. A 32 (1976) 751.
[27] P. Vajeeston, P. Ravindran, A. Kjekshus, H. Fjellvag, J. Alloys Compd. 450 (2008) 327–337.